AIMS Geosciences

AIMS Geosciences, 8(4): 706–717.
DOI: 10.3934/geosci.2022039
Received: 24 July 2022
Revised: 03 October 2022
Accepted: 19 October 2022
Published: 26 October 2022

http://www.aimspress.com/journal/geosciences

Research article

Calculation and determination of radioactivity in the old district of Najaf by using the track detector CR-39 and geographical information systems (GIS) methods

Adil A Mansoor and Hameed M Abduljabbar*

Department of Physics, College of Education for Pure Science Ibn-Al-Haitham, University of Baghdad, Baghdad, Iraq

* **Correspondence:** Email: hameed.m.aj@ihcoedu.uobaghdad.edu.iq; Tel: 9647801915114.

Abstract: This research aims to study the radiation concentration distribution of the old District of Najaf (Iraq), where 15 samples were taken from featured sites in the District, which represents archaeological, religious, and heritage sites. Track detector CR-39 was used to calculate the concentration of three different soil weights for each sample site after being exposed for a month. Geographical information systems (GIS) were used to distribute the radioactive concentration on the sites of the samples, where two interpolation methods, namely the inverse distance weight method (IDW) and the triangle irregular network method (NIT), to study the distribution of the radioactivity concentration. The study showed that the western part of the district, which includes the old cemetery and the areas adjacent to the Najaf water depression, are characterized by a relatively high amount of radioactivity concentration compared to the eastern part, which represent the residential areas, and for all sample weights.

Keywords: radiation; radon concentration; old district of Najaf; CR-39; GIS

1. Introduction

Humans are exposed to radiation permanently from two main sources: natural and made-man (artificial) sources, and nuclear radiation, which are released by charged particles, such as alpha particles and natural uranium [1–3], This type of radiations is what this study will focus on, as well as

uncharged particles and electromagnetic radiation that work to ionize and excite atoms and molecules. Living organisms, cells, tissues, and organs are affected by radiation and differ in their sensitivity and how they are affected by different types of nuclear radiation [1,3,4].

Since this information is gathered through aerial photography or satellite imaging, remote sensing and geographic information systems are among the most crucial techniques utilized to gather data on this topic [5,6]. Due to its highly analytical data, remote sensing technology is linked with geographic information systems. Applications utilizing these systems include earth observation, monitoring changes to land and water cover, managing land resources, mapping, and other applications are just a few of the many domains where geographic information systems (GIS) and remote sensing (RS) technologies [7].

Below, some of the previous studies that that studied radioactivity using nuclear methods (CR-39) and image processing are addressed.

N.K. Libeesh, et al. [8], used geochemical (XRF) and remote sensing (RS) in the Salem District (Pakkanadu, India) by collecting samples from different locations and utilized the visible near Infrared (VNIR) and Short Wave Infrared (SWIR) regions of the Advanced Spaceborne Thermal Emission and Reflection Radiometer (ASTER), to retrieve the different band combinations and determine the shielding efficiency by gamma rays in the energy range (0.015–15 MeV). Additionally, it was found that the dunite rocks are characterized by the maximum shielding properties.

Lubna A. Alasadi and Ali A. Abojassim [9], measure the natural radioactivity of the background gamma radiation produced by (238 U, 235 U, 232 Th and 40 K), and the alpha emitters produced by (222 Rn, 226 Ra, and 238 U) in the collected soil samples from the cities of Najaf and Kufa in the Najaf governorate. The radiological hazard index was determined due to gamma and alpha emitters from soil samples and maps were drawn by the geographic information system (GIS).

Nikezic and Yu [10], used a computer program developed to calculate the light scattered from an assembly of alpha particle tracks in a PADC film. The ray-tracing method was applied to simulate light propagation through the tracks. The distribution of the scattered light was found to be independent of the equilibrium factor between radon and its progeny.

Fuminobu Sato, et al. [11], developed a monitoring system for the sites of time-lapse recording from tracks formed on the surface of the solid-state nuclear track detector, by irradiating the CR-39 nuclear track detector with alpha particles, this irradiation of CR-39 clarified the process of track formation and created an image model for developing the track through image processing programs for the time-lapse image data. Following the track's development through image analysis and computational simulation of the incident of the energetic particles on CR-39, the incidence angle was used to reveal the formation of the track resulting from that fall.

Mostofizadeh A, et al. [12], used MATLAB software as a method to study edge detection and used nuclear track density CR-39. Experimental and statistical results showed that not only did each particular edge detection method affects the accuracy of measurements but considering the overlapping phenomenon -including double and triple tracks but also demonstrated a significant difference in accuracies across of the mentioned techniques before and after image enhancement.

Hadad, et al. in [13], used an automated counting system adopted on a high-resolution scanner and related image processing software to study the CR-39 detector, once the electrochemical etching was performed the CR-39 detectors were scanned and computed by a developed software (called NTC) with high accuracy.

Sa'ad R Yousif et al. [14], used the gamma-ray spectrum using Nal (TI) detector to calculate the radioactivity for samples of soil taken from the Badra oil field (Iraq). The rustles are subjected on the map using the GIS software with the datum WGS1984 by means of the IDW interpolation system.

This research aims to detect and determine radioactivity using nuclear methods (CR-39) track detectors and assist GIS, in the old Najaf discrete, which is the center of Najaf Province. We have chosen this topic of radioactivity due to its relevance in tourism and cancer risk. Additionally, these sites were focused on in this study to investigate their level of ionizing radiation. It included the use of two interpolation methods, namely, the IDW and TIN [15,16], in studying the distribution of radioactivity concentration from the point and behavior bulk and its effect on determining the most radioactive areas.

2. The study area description

The old District of Najaf was chosen as a study area to measure the radioactivity concentrations of radioactive radon gas, which is located in Najaf Province, southwest of the capital Baghdad (Iraq). The study area is in (31º57′8.08 N to 32º7′34.86 N) latitudes and (44º5′0.45 E to 44º22′53.57 E) longitudes, as it is characterized by the flatness of the land. It contains distinctive sites such as the Cemetery (Wadi Al-Salam), and the areas adjacent to the Najaf water depression. It is a shrine for many citizens because it contains religious sites, including the shrine of Imam Ali. The urban areas are located on the eastern side of the district, with little urbanization in the western site [4,17], as shown in figure 1.

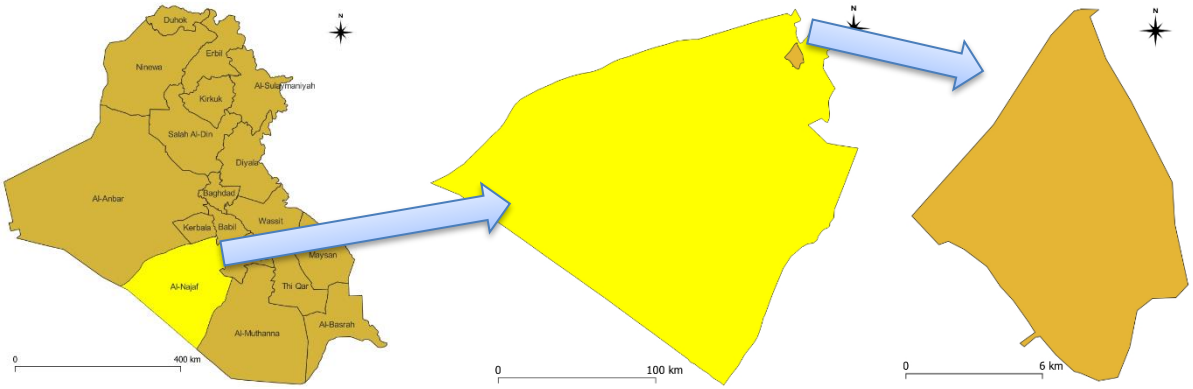

Iraq Shape Najaf Provence The Old City Shape

Figure 1. The study area location.

3. Material and methodology

In this research, the CR-39 nuclear track detector was used for the purpose of calculating the concentration of radon gas. The CR-39 detector was discovered in 1978 by (Cartwright & Shirk) at the University of California, USA, and it is one of the organic nuclear track detectors, and its molecular formula ($C_{12}H_{18}O_7$) is symbolized by (CR) [3,4,17], which is an abbreviation of (Columbia Resin), its density is (1.32 gm.cm^{-3}) and it has an ionization potential of (70.2 eV) and it is insoluble in chemical solvents [1,18,19]. The CR-39 detector is one of the best-recorded detectors for nuclear tracks, due to its characteristics [1,19,20].

Its high sensitivity to radiation (alpha particles, protons, and neutrons) and different energies, as well as its ability to record the effects of returning protons, resulting from their collision with neutrons

with high energies ranging between (0.1–20 Mev) [18]. This makes this detector sensitive to fast moving neutrons. In addition to optimal detector sensitivity, the detector exhibits the following benefits:

- High analytical ability.
- Sheer optical.
- Not dissolved in chemical solutions abrasive. If the abrasive solution works to break the polymeric chains and reduce their thickness.
- Highly homogeneous.
- Insensitive to big doses of gamma-rays and x-rays.
- Low cost and easy to use.
- Thermally hard material, the refractive index is lower than that of glass.

It is not affected by atmospheric factors such as temperature and humidity when stored for long periods under natural conditions, and it does not dissolve in chemical solutions, but decomposes through a decrease in its thickness during the chemical etching process. So, the following steps were taken.

- 15 samples of soil are collected from the Najaf province (Old a Najaf District) (Iraq). At depth of (15 cm).
- The samples are cleaned of impurities and dried in an electric oven for 2 hours, then grind to a fine powder in a (250 μm) sieve.
- Using the nuclear track detector CR-39, with a thickness of (500 μm) and dimensions of (1 × 1 cm^2), as shown in figure 2.

Figure 2. CR-39 detector.

- (10,20,30) grams of the soil sample is adopted to calculate nuclear radioactive concentration using a cylindrical cup with a length of (7 cm and 5 cm in diameter).
- Fixing the CR-39 detectors of the 1 cm^2 area at the top of the cup to prevent the alpha particles emitted from the Thoron gas Rn^{220} from reaching the detector.
- The soil samples are lefts for 1 month as exposure time.
- The CR-39 detector is Etched chemically using a NaOH solution by (6.25 N) at (60 ℃) for (4 hours).

The radiation background of the detector was measured. They were placed in an empty test tube of samples and sealed in the same manner and for the same time periods, in order to obtain the actual density of the effects of the alpha particles emitted from the samples under study without the impact of the surrounding environment.

Optical microscope with a magnification of (400 X) was used to count the average tracks of ten locations on the detector surface, the density of the track can be calculated by the following equations (1–3).

$$The\ track\ density(\rho) = \frac{Avarage\ number\ of\ the\ total\ track}{Area\ of\ field\ view}\ \left({}^{track}/_{mm^2}\right) \quad (1)$$

The detector (CR-39) was calibrated with a radium standard source Ra^{226}. Which emits radon Rn^{222} at a concentration (A = μCi = 18.5×10^4 Bq).

Calculated the radon concentration in samples by using an equations (1) and (2).

$$C_x = C_S\left({}^{\rho_x}/_{\rho_s}\right) \quad (2)$$

C_x: Is the concentration in the samples, C_s: Is the concentration in the standard sample.
ρ_x: Is the density of tracks in the unknown sample with (track/mm^2) and ρ_s: density of tracks in the standard sample with (track/mm^2).

$$C_{Rn} = \frac{\rho}{\eta T} \quad (3)$$

Where C_{Rn} is radon concentration ($Bq \cdot m^{-3}$) (ρ) is the track density (track$\cdot$mm^{-2}), T is the exposure time (day), and (η) is the calibration coefficient of CR-39 nuclear track detectors obtained from the experimental calibration $\left(0.2568\ {}^{tracks.mm^{-2}.day^{-1}}/_{Bq.m^{-3}}\right)$ of radon [1,2,17].

Calculating the radioactivity for each study area based on the calculated values for the sample areas using the two interpolation methods, the IDW method, and the TIN method.

4. Results and discussion

The study applied to the old Najaf District by selecting 15 sample sites within it, the chosen sites tend to be primarily religious, archaeological, and heritage landmarks. They were distributed over the district at an almost equal inter-distance to ensure the covering of the district. The locations of chosen sites were located using the UTM WGS84 38N projection system. Note that the study area was divided into four main areas, represented by the urban area, which represents the largest part, the old cemetery area, the plant areas, and areas with a small population density. The small population density areas can be considered uninhabited compared to the urban area, as illustrated in Table1 and figure 2 a,b.

The radioactivity concentrations were calculated for each site according to the steps shown in the methodology, where the drying and grinding process was carried out to a granular size of 250 μm, and the exposure process was performed for 30 days from the soil to three different weights, as shown in figure 4.

Table 1. The location and description of the chosen sites.

Location Code	Coordinates		Description
	N	E	
S1	3540135	438435.2	Media Street (Al-Huwaish)
S2	3542565	436857.5	Najaf Museum
S3	3544725	435885.1	Shrine Safa al-Safi
S4	3546884	434804.6	Twentieth Revolution Square
S5	3549196	433665	Farm 1
S6	3547155	433155.2	Zine El Abidine Street
S7	3544809	433368.3	The Tomb of the Martyr Al-Sadr I
S8	3545385	431534.7	Gate 6 the Ancient Cemetery
S9	3544395	431294.8	Tosi Street Cemetery
S10	3542895	432014.7	Gate 2 the Ancient Cemetery
S11	3542446	433515.3	Al-Tusi Street
S12	3540735	434596.2	Gate 4 the Ancient Cemetery
S13	3539326	436245.2	Hawally Street (Albu Amer)
S14	3537315	437264.5	Hawally Street Cemetery
S15	3537795	438614.8	Second Ambassador farm

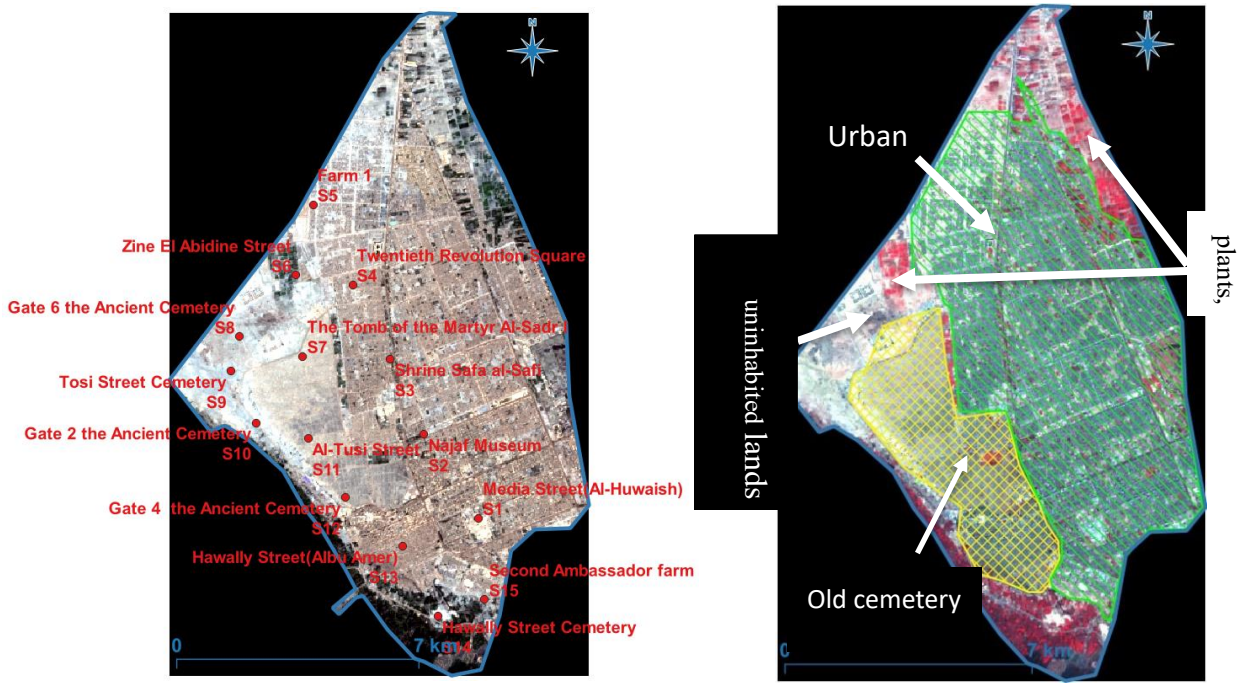

a b

Figure 3. Image of the old Najaf according to the administrative border (a) fixed on it the sample site location (b) urban, plants, the old cemetery, and uninhabited lands locations (Near Infrared, Red, Green).

Sodium hydroxide weighing

The etching solution with Normality of 6.25N

Water bath and detector etching process

Figure 4. Illustrate the detectors etching process.

The counting of the accumulated tracks on the track detector CR-39 was carried out using a light microscope with a magnification capacity of 400 X, where a counting rate of five places was taken in the detector, as illustrated in figure 5.

Optical microscope

Example of tracks image

Figure 5. Counting processing after etching.

Which covers most of the area of the detector, after which the impact density and radioactivity concentration was calculated for each site and according to the equations (1,3) for each site, as shown in Table 2. The radioactivity concentration weights for three weights are distributed over the study area, as illustrated in figure 6.

Table 2. The calculated tracks density and radon concentration.

Location Code	10 gm		20 gm		30 gm	
	Track density N. of (track· mm^{-2})	Radon Concentration (*Bq* · m^{-3})	Track density N. of (track· mm^{-2})	Radon Concentration (*Bq* · m^{-3})	Track density N. of (track· mm^{-2})	Radon Concentration (*Bq* · m^{-3})
S1	139.0533	18.04948786 ∓ 4	292.8994	38.01913399 ∓ 2.966479	381.6568047	49.54008369 ∓ 6.107373
S2	213.0178	27.65027927 ∓ 6.123724	281.0651	36.48300737 ∓ 4.159327	346.1538462	44.93170381 ∓ 2.345208
S3	233.7278	30.33850086 ∓ 3.646917	263.3136	34.17881743 ∓ 3.04959	431.9526627	56.06862185 ∓ 4.024922
S4	239.645	31.10656418 ∓ 3.271085	295.858	38.40316565 ∓ 4.449719	402.3668639	52.22830528 ∓ 4.658326
S5	286.9822	37.25107068 ∓ 4.062019	381.6568	49.54008369 ∓ 4.037326	420.1183432	54.53249522 ∓ 5.567764
S6	431.9527	56.06862185 ∓ 3.834058	440.8284	57.22071682 ∓ 3.04959	591.7159763	76.8063313 ∓ 4.827007
S7	393.4911	51.07621031 ∓ 4.658326	526.6272	68.35763486 ∓ 3.834058	671.5976331	87.17518602 ∓ 3.872983
S8	278.1065	36.09897571 ∓ 2.701851	281.0651	36.48300737 ∓ 2.701851	529.5857988	68.74166651 ∓ 7.402702
S9	349.1124	45.31573547 ∓ 3.834058	452.6627	58.75684344 ∓ 1.923538	426.035503	55.30055854 ∓ 7.95613
S10	281.0651	36.48300737 ∓ 3.577709	387.574	50.308147 ∓ 4.32435	405.3254438	52.61233694 ∓ 5.338539
S11	346.1538	44.93170381 ∓ 5.700877	363.9053	47.23589375 ∓ 5.974948	470.4142012	61.06103338 ∓ 3.847077
S12	369.8225	48.00395706 ∓ 3.646917	508.8757	66.05344492 ∓ 4.743416	597.6331361	77.57439461 ∓ 2.915476
S13	298.8166	38.78719731 ∓ 4.494441	384.6154	49.92411534 ∓ 4.929503	526.6272189	68.35763486 ∓ 6.870226
S14	319.5266	41.4754189 ∓ 6.300794	420.1183	54.53249522 ∓ 4.636809	523.6686391	67.9736032 ∓ 5.244044
S15	322.4852	41.85945056 ∓ 3.577709	428.9941	55.68459019 ∓ 4.560702	562.1301775	72.96601473 ∓ 4.505552

In order to find the effect of the amount of radioactivity concentration calculated for the location of the samples on the rest of the study areas, the interpolation method was performed using inverse distance weight (IDW), and the method of interpolation using the triangle

Irregular network (TIN), where we note in general the division of the study area into two parts in terms of the intensity of radioactivity in the region on the western side of the study area, characterized by a relatively high concentration of radioactivity compared to the eastern region and the various weights that were relied upon.

The use of IDW allows us to deal with the sites that were selected in the study area as point

sources where the radioactivity is concentrated and whose effect is transmitted to the neighboring areas in a radioactive manner. The increase in weight of the soil sample confines the area of high radioactivity in areas The Tomb of the Martyr Al-Sadr I and Gate 4 the Ancient Cemetery and two valleys located in the ancient cemetery of Najaf Wadi Al-Salam), then the use of 10 g of soil showed that all the areas of the western samples in the study area have radioactivity. High compared to nearby areas, as shown in figure7.

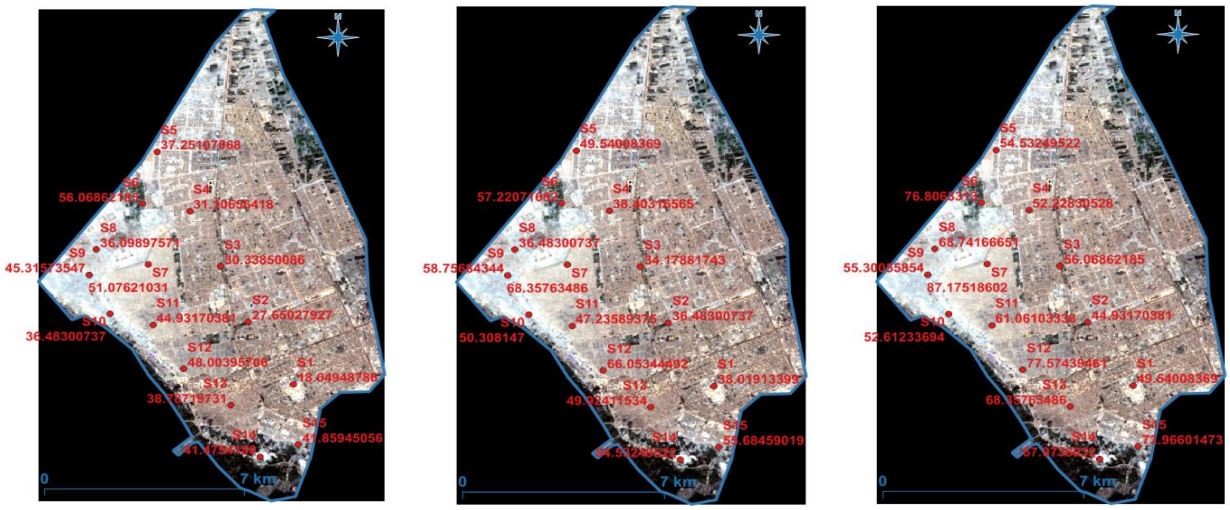

10 gm 20 gm 30 gm

Figure 6. The distribution of the radioactivity concentration over the study area and for the three weights.

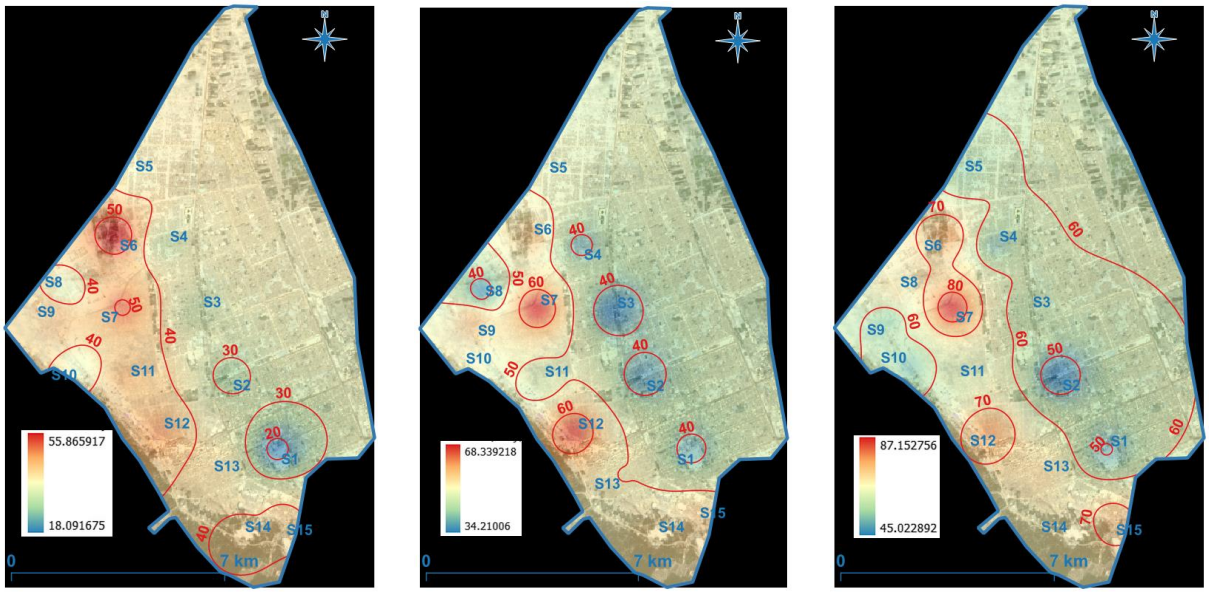

10 gm 20 gm 30 gm

Figure 7. The IDW interpolation results for different sample weights.

The use of the IDW interpolation system does not describe the distribution of the concentration of the radioactivity area, as the distribution of the soil samples that were taken are part of the geological

and environmental reality of the study area, and therefore the correlation between the sites of the samples to study the concentration of radioactivity must be taken into account. Thus, the use of (TIN) enabled us to calculate the amount of radioactivity concentration for each region confined between the nearest three points, to show the distribution of radioactivity in the form of regions, not as point sources, which is closer to the normal behavior of the distribution of radioactivity, as shown in Figure 4. Where we notice an increase in the concentration of radioactivity in the western regions of the study area, specifically in the area of the old Najaf cemetery (Wadi Al-Salam) and the areas adjacent to the increasing amount of soil used in calculating the concentration of radioactivity reduced the difference between high and low areas in terms of radioactivity concentration, but it did not change the radioactivity concentration sites in the old cemetery area and the areas adjacent to the Najaf water depression, as shown in figure 8.

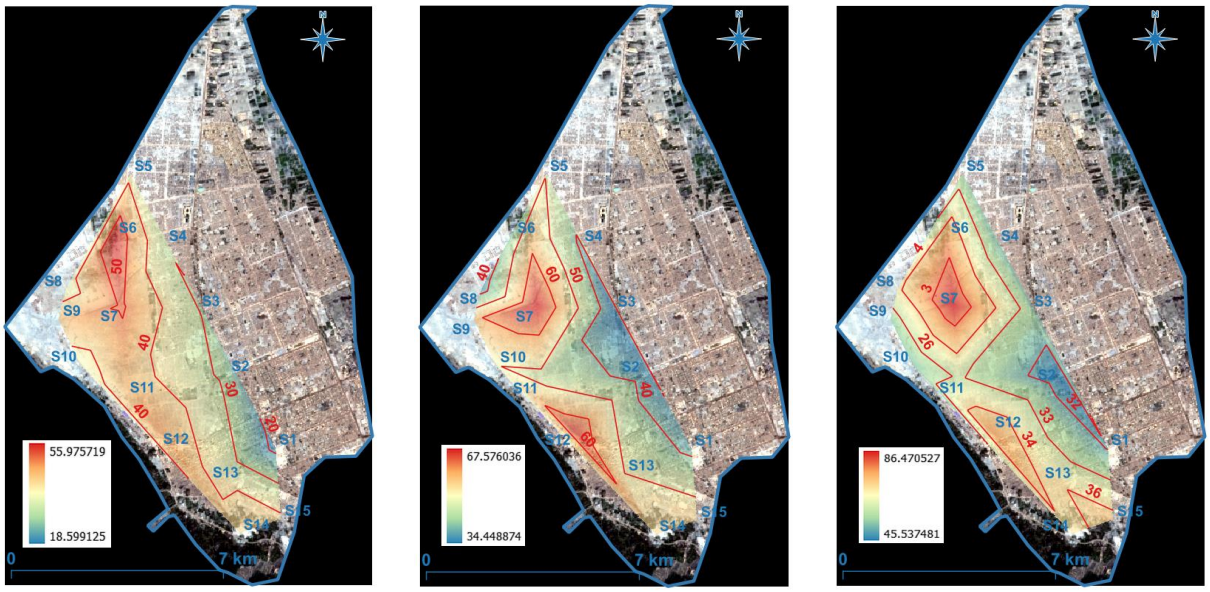

10 gm 20 gm 30 gm

Figure 8. The TIN interpolation results for different sample weights.

5. Conclusions

Depending on the results we can drive the following conclusions: (1) The relative increase in radioactivity concentration in the study area's western region, which is the old cemetery of (Wadi Al-Salam) and the adjacent areas of the Najaf water Depression and lower in the eastern residential areas. (2) The use of low weights leads to a difference in the concentration of radioactivity between the different sampling areas, which decreases with increasing the amount of soil. (3) The use of the interpolation method TIN is more realistic and closer to the real distribution of the concentration of radioactivity because it deals with it on a bulk basis, unlike the method IDW, which deals with it on a point source basis.

Conflict of interest

The authors declare no conflict of interest.

References

1. Hussein DAS, Measurement of Radon Concentrations in College of Education/Ibn Al-Haitham Buildings Using CR-39 Detector and RAD-7 Monitor. Baghdad: College of Education/Ibn Al-Haitham, University of Baghdad, 2018.
2. Mahdi KH, Subhi AT, Sharif NR, et al. (2018) Determination of Radon Concentrations in Soil Around Al-Tuwaitha Site Using CR-39 Detector. *Eng Technol J* 36: 108–112. http://dx.doi.org/10.30684/etj.36.2C.2
3. Saed BM (1998) *Determination of radon concentration in buildings by using the nuclear track detector CR-39*. College of Education. Ibn Al- Haitham, University of Baghdad.
4. Tawfiq NF, Nasir HM, Khalid R (2018) Determination of Radon Concentrations in AL-NAJAF Governorate by Using Nuclear Track Detector CR-39. *ANJS* 15: 83–87. https://doi.org/10.22401/JNUS.15.1.12
5. Mohammad GM (1994) *Land use mapping of selected areas of county Durham, north-east England, by satellite remote sensing and field survey methods*. Durham University.
6. Congalton RG, Fenstermaker LK, Ensen JR, et al. (1991) Remote sensing and geographic information system data integration: error sources and Research Issues. *Photogramm Eng Remote Sens* 57: 677–687.
7. Jha MK, Chowdary VM, Peiffer S (2017) Groundwater management and development by integrated remote sensing and geographic information systems: prospects and constraints, CRC Press. *Water Resour Manage* 21: 427–467. https://doi.org/10.1007/s11269-006-9024-4
8. Libeesh NK, Naseer KA, Arivazhagan S, et al. (2022) Characterization of Ultramafic–Alkaline–Carbonatite complex for radiation shielding competencies: An experimental and Monte Carlo study with lithological mapping. *Ore Geol Rev* 142: 104735. https://doi.org/10.1016/j.oregeorev.2022.104735
9. Alasadi LA, Abojassim AA (2022) Mapping of natural radioactivity in soils of Kufa districts, Iraq using GIS technique. *Environ Earth Sci* 81: 279. https://doi.org/10.1007/s12665-022-10407-8
10. Nikezic D, Yu KN (2009) Light scattering from an assembly of tracks in a PADC film. *Nucl Instrum Methods Phys Res Sect A* 602: 545–551. https://doi.org/10.1016/j.nima.2009.01.204
11. Sato F, Kuchimaru T, Kato Y, et al. (2008) Digital image analysis of etch pit formation in CR-39 track detector. *Jap J Appl Phys* 47: 269–272.
12. Mostofizadeh A, Sun X, Kardan MR (2008) Improvement of nuclear track density measurements using image processing techniques. *Am J Appl Sci* 5: 71–76.
13. Tilehnoee Hadad K, Hakimdavoud MR, Hashemi-Tilehnoee M (2011) Indoor radon survey in Shiraz-Iran using developed passive measurement method. *Iran J Radiat Res* 9: 175–182.
14. Yousif SR, Abojassim AA, Hayder A (2019) Mapping of natural radioactivity in soil samples of badra oil field project using GIS program. *Nucl Phys Energy* 20: 60–69.
15. Abduljabbar HM, Abdul IM, Mahdia SH (2018) Measuring surface porosity for zirconium enforced by different additive rates of nanosilica by means of image processing. *AIP Conf Proc* 1968: 1–8. https://doi.org/10.1063/1.5039231
16. Marid HA, Jarallah NT, Abduljabbar HM (2018) Radioactivity effect on the shape ofd even-even nuclei for Uranium and thorium series. *Results Phys* 11: 406–409. https://doi.org/10.1016/j.rinp.2018.06.024
17. Mahdi KH (2006) *Identification and Measurements of Natural and Industrial Radioactive Pollutants in Environment of Baghdad City Using Gamma Spectrometry and Solid State Nuclear Track Detector CR-39*. Baghdad: College of Education/Ibn Al- Haitham, Baghdad University.

18. Subhi AT (2013) Calculation of the concentrations of depleted uranium in the diyala river sediment samples using the nuclear track detector CR-39. *Ibn Al-Haytham J Pure Appl Sci* 26: 122–131.
19. Mohammed NA, Calculation of the Specific Activity of Radionuclides in Soil and Radon Concentration and its Health Effects in, Baghdad: Collage of Education for Pure Science-Ibn Al Haitham, University of Baghdad, 2020.
20. Ishnayyin HG, Find an Empirical Formula for Indoor Radon Measurement Emitting from Building Materials. Baghdad: College of Education/Ibn Al- Haitham, Baghdad University, 2015.